

Value of Hydro Power Flexibility for Hydrogen Production in Constrained Transmission Grids

Espen Flo Bødal and Magnus Korpås

*Department of Electric Power Engineering
Norwegian University of Science and Technology - NTNU
O. S. Bragstads plass 2E, 7034 Trondheim, Norway
E-mail: espen.bodal@ntnu.no*

Abstract

The cost of large scale hydrogen production from electrolysis is dominated by the cost of electricity, representing 77-89 % of the total costs. The integration of low-cost renewable energy is thus essential to affordable and clean hydrogen production from electrolysis. Flexible operation of electrolysis and hydro power can facilitate integration of remote energy resources by providing the flexibility that is needed in systems with large amounts of variable renewable energy. The flexibility from hydro power is limited by the physical complexities of the river systems and ecological concerns which makes the flexibility not easily quantifiable. In this work we investigate how different levels of flexibility from hydro power affects the cost of hydrogen production.

We develop a two-stage stochastic model in a rolling horizon framework that enables us to consider the uncertainty in wind power production, energy storage and the structure of the energy market when simulating power system operation. This model is used for studying hydrogen production from electrolysis in a future scenario of a remote region in Norway with large wind power potential. A constant demand of hydrogen is assumed and flexibility in the electrolysis operation is enabled by hydrogen storage. Different levels of hydro power flexibility are considered by following a reservoir guiding curve every hour, 6 hours or 24 hours.

Results from the case study show that hydrogen can be produced at a cost of 1.89 €/kg in the future if hydro power production is flexible within a period of 24 hours, fulfilling industry targets. Flexible hydrogen production also contributes to significantly reducing wasted energy from spillage from reservoirs or wind power curtailment by up to 56 % for 24 hours of flexibility. The results also show that less hydro power flexibility results in increased flexible operation of the electrolysis plant where it delivers 39-46 % more regulating power, operates more on higher power levels and stores more hydrogen.

Keywords: Power System Analysis, Hydro Power, Wind Power, Large Scale Hydrogen Production, Energy Storage

1. Introduction

In 2015, 96% of all hydrogen production was based on fossil energy sources such as natural gas, coal and oil, resulting in a significant carbon footprint[1]. Natural gas is the largest energy source for fossil hydrogen production with 46 % of the global market. To reduce the carbon footprint of hydrogen production from natural gas, CO₂ can be captured from the production process using steam-methane reforming (SMR). SMR has a typical capture rate of 90% of the produced CO₂, reducing emissions from 9.26 to 0.93 kg CO₂/ kg H₂ according to case studies by the National Renewable Energy Laboratory (NREL) [2]. NREL estimates the current prices of large-scale hydrogen production from natural gas with with carbon sequestration at 340 ton/day to be 1.56 \$¹/kg in 2015, for a plant starting up in 2040 the costs increase to 1.72 \$/kg H₂ due to higher feed stock costs as a result of higher natural gas prices.

The other commercial option for hydrogen production is to produce hydrogen by electrolysis, using either alkaline, proton exchange membranes (PEM) or solid oxide (SO) electrolysis

[3]. Alkaline and PEM electrolysis are mature technologies, while SO is still in the R&D-phase. The carbon footprint of hydrogen produced from electrolysis depends on the emissions of the electricity source, if the electric power used for the electrolysis is renewable, such as solar, wind or hydro power, the hydrogen has a very low carbon footprint.

The largest electrolysis plant for hydrogen production installed in history was used to produce ammonia for use in fertilizer at Rjukan in Norway with a capacity of 60 ton/day [3], which would amount to about 130 MW of electric load using today's alkaline electrolyzers. Currently an electrolysis plant is under planning in connection to Rhineland refinery in Germany and will be the largest electrolysis plant in the world for hydrogen production with a capacity of about 3.6 ton/day [4].

Small scale wind-hydrogen systems are extensively studied in the past and several test facilities are in operation as for example at Utsira in Norway [5] and other countries such as United States, Canada, Germany, Italy, Finland, United Kingdom, Japan, and Spain [6]. Different types of systems exist with different purposes, ranging from pure energy storage systems as at Utsira where hydrogen is stored and used in fuel cells to gen-

¹Monetary values from NREL cases are in 2016 dollars

Nomenclature

Indices

i, j	Bus
s	Second stage node
t	Time stage

Parameters

Δ	Price addition for import [$\text{€}/MWh$]
$\eta^{d/s}$	Conversion factor, power to hydrogen [MWh/Nm^3], directly or via storage
λ_t^s	Day-ahead price [$\text{€}/MWh$]
ρ_s	Probability of wind power scenario
C_t^d	Cost for deviating from schedual [$\text{€}/MWh$]
$C^{r/i}$	Cost of rationing [$\text{€}/MWh$] or hydrogen import [$\text{€}/Nm^3$]
$C^{v+/v-}$	Cost for violating end reservoir level [$\text{€}/MWh$]
D_{ti}	Electricity demand [MWh]
E_i^{max}	Capacity of electrolysis plant [MW]
H_t^D	Hydrogen demand [MWh]
H_i^{max}	Capacity of hydrogen storage [Nm^3]
I_{ti}	Inflow to hydro power reservoirs [MWh]
$P_{ti}^{min/max}$	Min or max power production [MW]
P_{tis}^w	Wind power scenario [MWh]
S^{ref}	Reference power for the system [MW]
T_{ij}^{max}	Transmission capacity from bus i to j [MW]
$V_i^{0/max}$	Initial volume or max capacity for reservoir [MWh]
X_{ij}	Reactance between bus i and j [$p.u.$]
Sets	
\mathcal{B}	All buses

C_i	Buses connected to bus i by transmission lines
$\mathcal{H}, \mathcal{W}, \mathcal{P}, \mathcal{H}_2$	Hydro power, wind power, all power plants or hydrogen plants
\mathcal{M}	Market Bus
\mathcal{N}	Normal buses (excl. market bus)
\mathcal{S}	Wind Power Scenario
\mathcal{T}	Time stages

Variables

δ_{tis}	Voltage phase angle at bus
c_{tis}	Energy curtailment [MW]
$d_{tis}^{exp/imp-/+}$	Negative/ positive change in export/ import [MW]
$d_{tis}^{H_2-/+}$	Negative/ positive change in hydrogen production [MW]
$d_{tis}^{hydro-/+}$	Negative/ positive change in hydro power production [MW]
f_{tj}	Power flow from bus i to j [$p.u.$]
h_{tin}^d	Hydrogen directly from electrolysis [Nm^3]
h_{tis}^{imp}	Hydrogen imported/ not served [Nm^3]
h_{tin}^p	Hydrogen to storage [Nm^3]
h_{tin}^s	Hydrogen from storage [Nm^3]
h_{tin}	Hydrogen storage level [Nm^3]
$p_{tis}^{imp/exp}$	Power import or export [MW]
p_{tis}	Production [MW]
r_{tis}	Rationing of power [MW]
s_{tin}	Spillage/ bypass of water [MWh]
$v_n^{+/-}$	Violation of end reservoir level [MWh]
v_{tin}	Reservoir level [MWh]

erate electricity at a later time to systems where hydrogen is produced as a product for use as fuel or in industrial processes known as power-to-gas [7]. Hydrogen storage solutions are increasingly considered as alternative to electric power grid upgrades in rural areas with weak or no grid connections such as the islands communities along the Norwegian Coast, the Faroe Islands and Svalbard [8, 9, 10, 11].

For a large-scale electrolysis plant built in 2015 with PEM electrolyzers and a production capacity of 50 ton/day the hydrogen production cost estimated by NREL was 5.18 \$/kg, while a for a plant built in 2040 it is 4.48 \$/kg. The expected reduction in hydrogen production cost is due to a reduction in total capital costs of about 60 %, whereof the cost of electrolyzers are assumed to be reduced from 900 to 400 \$/kW in line with observations and expert expectations [12]. The share of the to-

tal production costs that arise from electricity consumption thus increase from 77.2 % to 88.5%, while the electricity price is assumed not to be significantly different in this case. This shows that the price of hydrogen production from electrolysis is going to be even more heavily influenced by the electricity price in the future as the capital cost of electrolysis is reduced [13]. The US Department of Energy (DoE) estimated the cost of alkaline electrolysis to be 4.75 \$/kg in 2011 and set targets of 3.47 and 2.32 \$/kg in 2015 and 2020 respectively. The DOE cost targets for hydrogen production include a significant reduction in electricity price from to 0.073 \$/kWh in 2011 to 0.057 and 0.036 \$/kWh for 2015 and 2020 respectively[14].

To lower the cost of electrolytic hydrogen production the electrolysis facility need to be located in a area with low electricity costs. The cost of renewable energy technologies such as

wind and solar power has dropped significantly the latest years and are now competitive with producing electricity from coal and other fossil sources [15]. The areas with the best conditions for producing renewable electricity is often located far from consumers and are not developed due to the large costs of constructing transmission lines [16]. This creates areas with low-cost clean electric energy that is "trapped" due to its location and insufficient transmission infrastructure such as western China [17], the North-Sea region [18] or western Texas [13]. Producing hydrogen in these areas can be a way to utilize these energy sources without building costly transmission lines [19, 20, 21]. However, there are still significant costs associated with transporting hydrogen to consumers, but it can be done in a more flexible way in the form of gaseous hydrogen, liquefied hydrogen or ammonia on ships, trucks or in pipelines.

To produce hydrogen in an area with a lot of intermittent renewable energy we need extra electrolysis capacity and hydrogen storage. Hydrogen storage allows the hydrogen production plant to run flexibly to counteract the variations in electricity produced from renewable sources [22]. This flexibility allows for integration of more renewable energy, has significant value to the electric power system [23] and is a popular topic in electric power system research [24].

Rolling horizon is a framework for optimization models where the same model is solved sequentially with a constant horizon, the parameters are updated and are dependent on the solution of the previous instance of the model. This framework is frequently used when studying integration of renewable energy and the regulating market. The sequential temporal structure of the rolling horizon framework is a realistic way to simulate how energy markets work in practice and gives a good representation of the challenges arising from renewables resulting in more uncertainty in power system operation [25], flexible hydrogen production [26] or energy storage management [27]. Rolling horizon based models are more computationally tractable than more sophisticated scenario-tree based models that often requires parallel computing on high performance computers to allow for detailed modelling of large power systems [28].

The value of flexible hydrogen production is dependent on other sources of flexibility in the power system. In systems dominated by hydro power with reservoirs there are potentially a lot of available flexibility as water can be stored for later. However, it is not obvious to which extent hydro power producers will be able to deliver flexibility due to the complexity of the waterways, variation in inflow and grid constraints. In this paper, we investigate the impact short-term hydro power flexibility has on the value of flexible hydrogen production.

The rolling horizon modelling framework presented in this paper is a further development of previous work [29] and includes the combination of power flow, long-term hydro power storage and short-term hydrogen storage in addition to short-term wind power uncertainty. In this work we focus on shorter term uncertainties, and leave out the long-term uncertainty and some of the modelling details. The long-term uncertainty can have a significant impact on the the hydro power strategies, but the problem would be intractable when considering both long

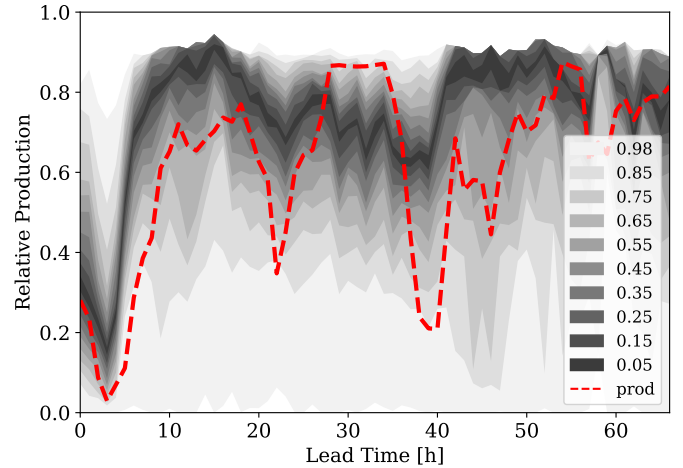


Figure 1: Example of a quantile forecast. The different colors represents probability intervals for the wind power production for a given hour ahead in time. The green line represents the actual production that occurred.

and short-term uncertainties in the same optimization model. The market structure of the current electric power system is included, modelled as a two-stage optimization problem with a day-ahead market and a simplified model of the real-time balancing market. The regional power system is modelled with a detailed grid description, including electric loads, hydro power plants, wind power plants, and a facility for large-scale electrolysis and hydrogen liquefaction.

In Section 2 we explain the main parts of the model, which can be grouped into three parts; how the wind power scenarios are generated, the two-stage optimization model and the rolling horizon framework. The case study of a remote area in northern Norway is presented in Section 3. In Section 4 the results from the case study are presented and discussed, while the conclusions are given in Section 5.

2. Method

2.1. Wind Power Forecasting

Numerical weather predictions and historical observations of produced wind power are used to create quantile forecasts as shown in the example in Figure 1. This is done by using wind speeds and directions from weather forecasts made by The Norwegian Meteorological Institute [30] and recorded production by the Norwegian Water Resources and Energy Directorate [31] in a local quantile regression algorithm as described in detail in [32]. The local quantile regression is formulated as a linear optimization problem as described in [33] and solved. One optimization problem has to be solved for each wind power plant, quantile and lead-time resulting in solving a lot of small optimization problems for making one quantile forecast.

From the quantile forecast we can sample wind power scenarios [34], in short we use the historical production records to create a correlation matrix for spatial and temporal correlations and sample scenarios from a multivariate normal distribution which is transformed into wind power scenarios using

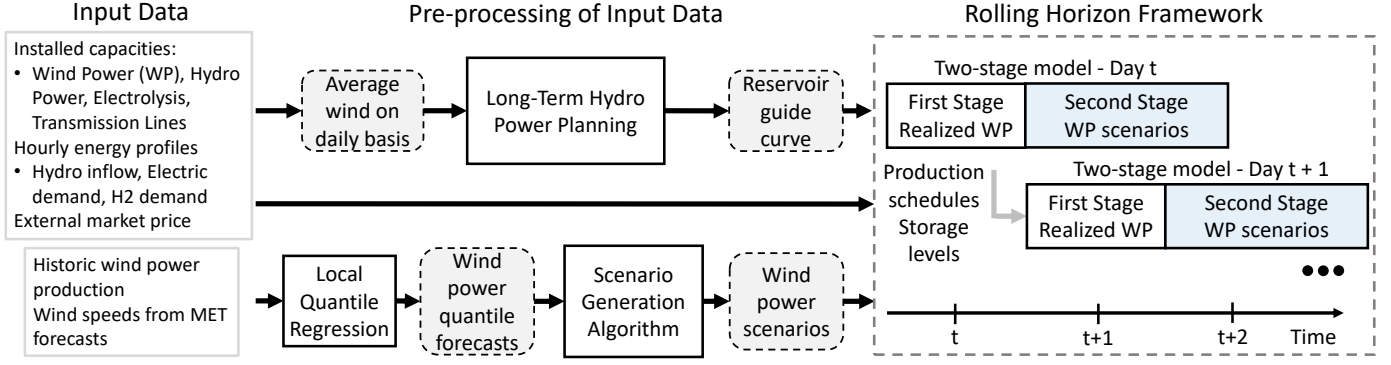


Figure 2: Illustration of the input data, modelling steps and rolling horizon framework

the cumulative gaussian normal distribution and the cumulative distribution function (cdf) of the quantile forecasts.

2.2. Rolling Horizon Framework

For each day in the rolling horizon algorithm an two-stage optimization problem is solved. The two stages are replicating the structure of the Nordic electric power market [35] and are illustrated in Figure 2. In the first stage, we are following a production schedule that was made the day before, while making the needed adjustments as one would in the regulating power market to balance supply and demand of electricity. The hour-to-hour adjustments to the production schedule comes at a higher cost, representing a premium of readiness related to costs that arise for delivering power on short notice [36].

The production schedule that is followed in the first stage represents the day-ahead market bids, where producers make a optimal dispatch based on the information they have the day before the actual operational day. We assume that the producers are risk-neutral, such that the day-ahead generation schedule is the one that gives the lowest expected costs considering a set of scenarios for wind power production.

The production schedule for the next day is represented by the first 24 hours of the second stage. This schedule is sent to the next two-stage problem as the rolling algorithm moves on to the next iteration. The consecutive two-stage problems are connected through these production schedules, the storage levels in the hydrogen storage and reservoirs, which are passed between them in the rolling horizon algorithm. In this way the rolling horizon algorithm rolls through the year, with a separate two-stage problem representing each day where they all are connected by passing on information about generation schedules and storage levels. This gives a realistic representation of how the system is operated as it preserves the chronology of information, such as how much wind power we expect tomorrow at a given instance in time.

2.2.1. Long-Term Strategy

As hydro power reservoirs can store water for many years the short-term scheduling horizon of the rolling horizon model, which is in the range of several days to a couple of weeks, is too short to determine a good reservoir operation strategy. Thus

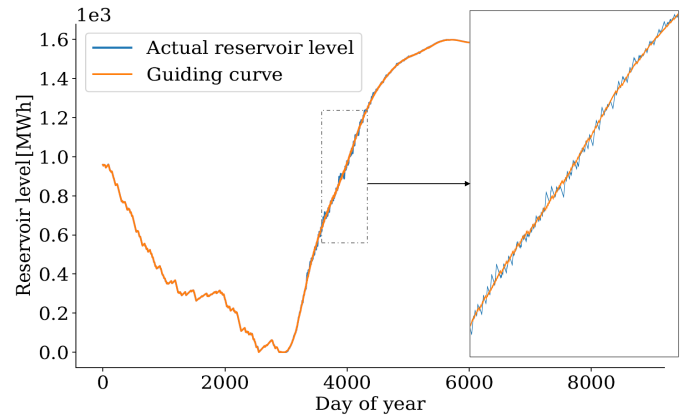


Figure 3: Example of the reservoir level following the guiding curve for long-term hydro power management.

a long-term strategy needs to be an input to the rolling horizon model, there are several ways to implement this strategy and here we use guiding curves as shown in Figure 3, meaning an input reservoir level that has to be reached at specified times e.g. the end of the day. This gives the rolling horizon model the opportunity to use hydro power as a source of flexibility in the short-term, while also considering a long-term strategy. The intra-day variations from the guiding curve look small due to the large amount of energy stored in the reservoir, but have a significant impact on the result. A more sophisticated method would be to use a water-value matrix [37, 38], setting the marginal value of the water at different times and reservoir levels, but this is more complicated and not the focus of this work.

The combination of modelling short-term stochastic properties of renewables and flexibility from resources with both short and long-term storage in a tractable way separates this work from previous work on integration of renewables or hydrogen production, that usually focus either on short-term dynamics or long-term trends.

2.3. Regional Power System Operation

The mathematical formulation of the two-stage optimization problem is presented in the following equations. The objective

is given in Equation 1 and represents the optimal operation of a region of the power system. The objective is to find a solution that minimize the operational costs of supplying regional electric and hydrogen loads that are given by load-profiles. This is equivalent to maximizing the profit from selling power to the rest of the system, represented by the market bus ($i = 0$). For simplicity of notation the first stage is included in the set of scenarios or nodes with a probability of one ($\rho_0 = 1$).

$$\begin{aligned} \max \sum_{s \in \mathcal{S}} \rho_s & \left[\sum_{t \in \mathcal{T}} \left[\lambda_t^s p_{i0s}^{imp} - (\lambda_t^s + \Delta) p_{i0s}^{exp} - \sum_{i \in \mathcal{N}} C^r r_{iis} - \sum_{i \in \mathcal{H}_2} C^i h_{iis}^i \right. \right. \\ & - \sum_{i \in \mathcal{H}_e} C_t^d (d_{iis}^{H_2^-} + d_{iis}^{H_2^+}) - \sum_{i \in \mathcal{H}} C_t^d (d_{iis}^{hydro-} + d_{iis}^{hydro+}) \\ & - \sum_{i \in \mathcal{M}} C_t^d (d_{iis}^{exp-} + d_{iis}^{exp+} + d_{iis}^{imp-} + d_{iis}^{imp+}) \left. \right] \\ & - \sum_{i \in \mathcal{H}} (C^{v+} v_{is}^+ + C^{v-} v_{is}^-) \end{aligned} \quad (1)$$

In the two first terms of the objective function we have the power price, λ_t^s , times imports to, p_{i0s}^{imp} , and exports from, p_{i0s}^{exp} , the market bus, meaning income from exports from the system and costs of imports to the system respectively. An additional margin, Δ , is added to the power price for importing power to represent grid tariffs. The electric and hydrogen loads within the region have to be served, in the case the required load cannot be served penalties are included for rationing power, r_{iis} , and rationing/ importing hydrogen from other sources, h_{iis}^i , in the third and fourth term. The cost of deviating from the production schedule for the controllable units, hydro power, $d_{iis}^{hydro-/+}$, hydrogen loads, $d_{iis}^{H_2-/+}$, and import or export to the market bus, $d_{iis}^{exp/imp-/+}$, are included in the fifth, sixth and seventh term of the objective function. The final part of the objective function ensures that at the reservoir levels follow the long-term strategy described by the guiding curves for the hydro power reservoirs at specified times, any deviation, $v_{is}^{-/+}$, from the specified reservoir levels results in a penalty in the objective.

$$p_{iis} + c_{iis} = P_{iis}^w \quad \forall i \in \mathcal{W}, \forall t \in \mathcal{T}, \forall s \in \mathcal{S} \quad (2)$$

Wind power, P_{iis}^w , cannot be stored and has to be used for production of electricity, p_{iis} , when available or curtailed, c_{iis} , as stated in Equation 2.

$$v_{iis} = v_{(t-1)is} - p_{iis} - s_{iis} + I_{ti} \quad \forall i \in \mathcal{H}, \forall t \in \mathcal{T}, \forall s \in \mathcal{S} \quad (3)$$

$$v_{0is} = V_i^0 \quad \forall i \in \mathcal{H}, \forall s \in \mathcal{S} \quad (4)$$

$$v_{Tis} - v_{is}^+ + v_{is}^- = V_{T,i}^{curve} \quad \forall i \in \mathcal{H}, \forall s \in \mathcal{S} \quad (5)$$

Hydro power plants often have reservoirs and can store water to be used later, this is governed by the reservoir balance in Equation 3, where the reservoir level at the end of an time-step, v_{iis} , is equal to the reservoir level at the end of the previous time-step, $v_{(t-1)is}$, minus production, p_{iis} , and spillage, s_{iis} , plus the inflow to the reservoir, I_{ti} . The initial reservoir level, v_{0is} ,

is known and set by Equation 4 while the end reservoir level, v_{Tis} , should follow the long-term strategy given by the guiding curve, $V_{T,i}^{curve}$, as stated in Equation 5 or penalties will occur in the objective function.

$$h_{iis} = h_{(t-1)is} + h_{iis}^p - h_{iis}^s \quad \forall i \in \mathcal{H}_2, \forall t \in \mathcal{T}, \forall s \in \mathcal{S} \quad (6)$$

$$h_{iis}^d + h_{iis}^s + h_{iis}^i = H_{iis}^D \quad \forall i \in \mathcal{H}_2, \forall t \in \mathcal{T}, \forall s \in \mathcal{S} \quad (7)$$

The hydrogen plant also has a storage which is governed by the hydrogen storage balance in Equation 6. This is similar to the reservoir balance for hydro power reservoirs, the main difference is that loading of the hydrogen storage is governed by a decision variable for hydrogen production to storage, h_{iis}^p , as compared to the inflow in the reservoir balance which is a parameter and thus not controllable. Equation 7 is the hydrogen balance and makes sure the required amount of hydrogen is supplied to the hydrogen load, H_{iis}^D , either directly from the electrolyser, h_{iis}^d , from storage, h_{iis}^s , or imported from other sources, h_{iis}^i , at high costs.

$$\begin{aligned} \sum_{j \in \mathcal{P}_i} p_{rjs} - \eta^d h_{iis}^d - \eta^s h_{iis}^p - p_{iis}^{exp} \\ + p_{iis}^{imp} + r_{iis} = D_{ii} \end{aligned} \quad \forall i \in \mathcal{N}, \forall t \in \mathcal{T}, \forall s \in \mathcal{S} \quad (8)$$

The energy balance is shown in Equation 8 and states that produced energy from all sources connected to a bus plus imported electricity, p_{iis}^{imp} , has to be equal to the electricity needed to cover normal electric demand, D_{ii} , exported electricity, p_{iis}^{exp} , and electricity for hydrogen production, $\eta^s h_{iis}^p$ and $\eta^d h_{iis}^d$. If this is not the case, demand has to be rationed, r_{iis} , which represents a high cost. The energy demand for hydrogen production is divided into two parts, hydrogen produced directly to the hydrogen load, h_{iis}^d , or hydrogen produced to storage, h_{iis}^p , as hydrogen produced to storage demands more energy per unit of hydrogen due to compression to higher pressure.

$$\begin{aligned} d_{iis}^{H_2^-} - d_{iis}^{H_2^+} = \eta^d (h_{ii}^{d,plan} - h_{ii}^d) \\ + \eta^s (h_{ii}^{p,plan} - h_{ii}^p) \end{aligned} \quad \forall i \in \mathcal{H}_2, \forall t \in \mathcal{T}, \forall s \in \mathcal{S} \quad (9)$$

$$d_{iis}^{hydro-} - d_{iis}^{hydro+} = p_{ii}^{plan} - p_{iis} \quad \forall i \in \mathcal{H}, \forall t \in \mathcal{T}, \forall s \in \mathcal{S} \quad (10)$$

$$d_{iis}^{exp-} - d_{iis}^{exp+} = p_{ii}^{exp,plan} - p_{iis}^{exp} \quad \forall i \in \mathcal{M}, \forall t \in \mathcal{T}, \forall s \in \mathcal{S} \quad (11)$$

$$d_{iis}^{imp-} - d_{iis}^{imp+} = p_{ii}^{imp,plan} - p_{iis}^{imp} \quad \forall i \in \mathcal{M}, \forall t \in \mathcal{T}, \forall s \in \mathcal{S} \quad (12)$$

In Equation 9 and 10 variables are used to account for positive and negative deviations, $d_{iis}^{hydro-/+}$ or $d_{iis}^{H_2-/+}$, from the production schedules for hydro power production and hydrogen demand, p_{ii}^{plan} or $h_{ii}^{d,plan}$. Similar, Equation (11) and (12) accounts for deviations from the schedules for import, d_{iis}^{imp+} , and export, d_{iis}^{exp+} , from or to the market bus. In the first stage the

production schedules are a parameter-input from the previous run of the two-stage model, while for the second stage the production schedules are variables that are common for all scenarios (no s in the subscript) and determined by the optimization.

$$p_{ii}^{exp} - p_{ii}^{imp} = S^{ref} \sum_{j \in C_i} f_{ij} \quad \forall i \in \mathcal{B}, \forall t \in \mathcal{T}, \forall s \in \mathcal{S} \quad (13)$$

$$f_{ij} = \frac{1}{X_{ij}} (\delta_{tis} - \delta_{ijs}) \quad \forall j \in C_i, \forall t \in \mathcal{T}, \forall i \in \mathcal{B}, \forall s \in \mathcal{S} \quad (14)$$

The nodal flow balance in Equation 13 states that the sum of all power flows, f_{ij} , from a bus is equal to net power injected into the grid at that location, ie. the difference between power exported, p_{ii}^{exp} , and power imported, p_{ii}^{imp} . The power flow on each individual transmission line is dependent on the differences in voltage angle, δ_{tis} , between the two buses and the inverse of the line reactance, X_{ij} , as described by the dc power flow equation in Equation 14. The dc power flow equations are linearized versions of the full ac power flow equations and are widely used to represent power flow in large power system models [39]. Equation 15 to 19 states the upper and lower bounds for reservoir level, produced power, electrolyser power, hydrogen storage level and line flow.

$$0 \leq v_{tis} \leq V_i^{max} \quad \forall i \in \mathcal{H}, \forall t \in \mathcal{T}, \forall s \in \mathcal{S} \quad (15)$$

$$P_i^{min} \leq p_{tis} \leq P_i^{max} \quad \forall i \in \mathcal{H}, \forall t \in \mathcal{T}, \forall s \in \mathcal{S} \quad (16)$$

$$0 \leq \eta^d h_{tis}^d + \eta^s h_{tis}^p \leq E_i^{max} \quad \forall i \in \mathcal{H}_2, \forall t \in \mathcal{T}, \forall s \in \mathcal{S} \quad (17)$$

$$0 \leq h_{tis} \leq H_i^{max} \quad \forall i \in \mathcal{H}_2, \forall t \in \mathcal{T}, \forall s \in \mathcal{S} \quad (18)$$

$$-T_{ij}^{max} \leq f_{ij} S^{ref} \leq T_{ij}^{max} \quad \forall j \in C_i, \forall i \in \mathcal{B}, \forall t \in \mathcal{T}, \forall s \in \mathcal{S} \quad (19)$$

The model is implemented in Python using the PYOMO optimization package and solved with the GUROBI optimization solver. We run the model on a Dell Latitude E7470 laptop and the typical solution time is 6-7 hours for the case study.

3. Case study

The rolling horizon model is used in a case study for large-scale hydrogen production in Finnmark, northern Norway. The Region is illustrated in Figure 4 and has a constrained grid connection towards the south of Norway where most of the consumption is located. This region is a favorable region in Norway for on-shore wind power, but most of its potential is not developed due to transmission constraints. The installed wind power in this case study is set to be three times the present capacity. The hydrogen production facility is placed in bus 6 where there is currently a facility for production of liquefied natural gas. An overview of power plants, electric loads and transmission capacities are given in Table 1 and 3 based on data from the Norwegian Natural Resources and Energy Directorate [40] and Statistics Norway [41].

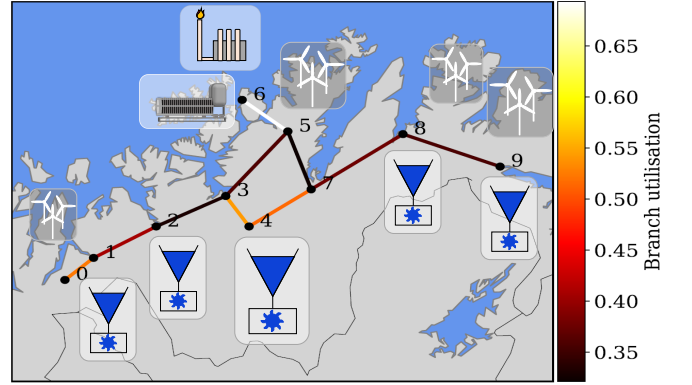


Figure 4: Illustration of the case study in Finnmark, northern Norway. Hydrogen production is located in node 6 with electrolysis, SMR and liquefaction. Buses 1, 5, 8 and 9 have wind farms and buses 1, 2, 4, 8 and 9 have hydro power plants. The size of the symbols indicate the installed capacities of each technology. The Transmission lines are colored with the average branch utilization.

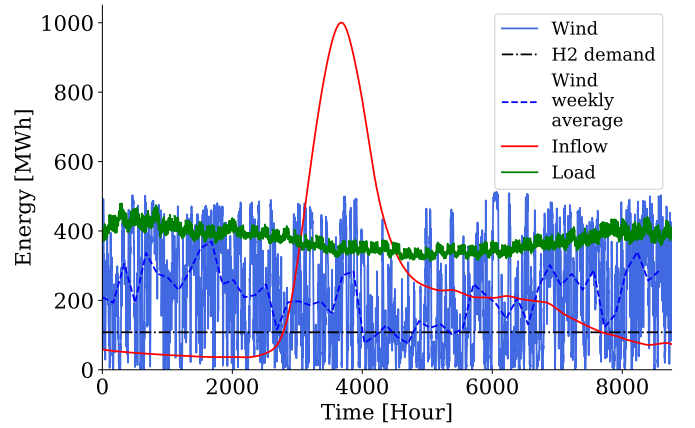


Figure 5: Profiles for the total energy available from wind and inflow or consumed by the electrical and hydrogen loads throughout 2015, used as input to the model.

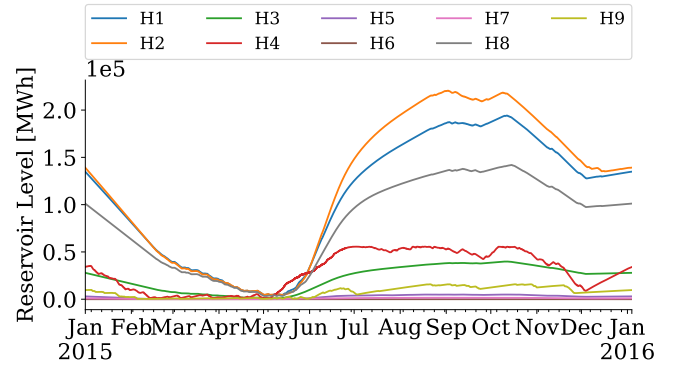


Figure 6: Long-term strategies for hydro power reservoirs according to bus number. The strategies are results from a long-term operational model for the system that uses perfect foresight of mean daily wind power.

Electric loads and market prices in the market bus are represented by historical data for 2015 from Nord Pool [42]. The total profiles for all available energy, wind and inflow, and demand, electricity and hydrogen, is shown in Figure 5. Weekly average wind power and electric load has a clear correlation with lower levels in the summer and higher levels in the winter, while hydro power inflow has a characteristic peak when the snow melts in the spring. The need for both short and long-term storage is apparent to be able to match the fluctuating wind energy and the peak in hydro power inflow with the demand profiles.

The guiding curves for the long-term hydro reservoir strategies are shown in Figure 6 and obtained from a deterministic operational model using average daily wind power. The electrolysis plant is assumed to serve a hydrogen demand of 50 ton/day, equivalent to a electric load of 108 MW, which would make it the largest electrolysis plant in the world for hydrogen production only comparable to the decommissioned Rjukan plant. The hydrogen demand is constant as it goes to a liquefaction plant that is assumed to be in constant operation.

In this case study we use installed capacities based on results from an deterministic investment model used for sizing of electrolysis capacity, hydrogen storage and installed wind power capacities for a given electric transmission grid scenario [43]. However, as shown in Table 3, the transmission capacities had to be significantly increased from the deterministic model output to avoid rationing as a result of introducing uncertainty from wind power. More electrolysis capacity is added to include more flexibility in the system. In summary the electrolysis capacity is 150 MW (2 894 kg/h) and hydrogen storage is 9 129 kg. This equals a minimum depletion time of the hydrogen storage of about 4.4 hours and a minimum filling time of 11.6 hours when considering the constant hydrogen load. The hydrogen plant can either serve the hydrogen load directly at a energy consumption of 51.8 kWh/kg or fill the storage at 53.3 kWh/kg at 350 bar [44]. The electrolysis plant is assumed be co-located with hydrogen production from natural gas, where the natural gas plant produces 450 ton/day based on steam-methane reforming (SMR). The hydrogen is liquefied and transported by ship to a region where energy is needed. The net energy demand for the SMR and liquefaction process is added to the load profile for bus 6 as a constant load at 164 MW, where the SMR process includes steam turbines resulting in a surplus of 14 MW electric power and the liquefaction demand of 178 MW.

Hydro power is allowed to deviate from the guiding curve within a certain interval of hours depending on the flexibility level without receiving any penalties as explained above. Six cases are considered in total by combining three different levels for hydro power flexibility for two different regulating price premiums (RP). The flexibility intervals are set to 0, 6 and 24 hours and denoted as low, medium or high hydro power flexibility. The regulating price premium is 15 and 30 % of the day-ahead price both for up and down regulation. It should be noted that these numbers are set higher than observed in the market today, which is typically around 10 % [36]. This is due to the relatively low amounts of wind power in the Nordic area compared to flexible hydro power, but may change as more variable

Table 1: Bus data for the case system. The electricity for hydrogen production and liquefaction is included in the bus 6 load. Liquefaction represent a constant load profile amounting to 1436 GWh/yr. The hydrogen production electric load profile is a result of the optimization with a total electricity demand of 946 GWh/yr.

Bus Nr.	Wind [MW]	Hydro [MW]	Reservoir [GWh]	Inflow [GWh/yr]	Load [GWh/yr]
1	10.0	80	224.8	303.6	225.5
2	0.0	85	231.9	363.5	35.1
3	0.0	17.7	46.5	92.3	374.3
4	0.0	145.2	56.7	894.6	22.7
5	200.5	4.2	5.0	16.4	121.5
6	6.7	1.1	0.0	3.0	2570.8
7	0.0	1.7	1.6	16.3	136.6
8	40.0	55.1	168.5	196.6	80.2
9	387.1	78.3	16.1	82.4	680.3
Sum	644.3	468.3	751.1	1968.7	4247.0

Table 2: Parameter input to the model in €/MWh. The electricity price series in market node is represented by the average value.

Mean electricity price	$\bar{\lambda}^s$	20.44
Rationing	C^r	5000
Guiding curve deviation	$C^{v+/v-}$	50
Hydrogen import	C^i	6000
Regulating cost [% of spot price]	C_t^d	0.15/0.30

wind power is integrated into the power system and more flexibility is needed for balancing supply and demand of electricity [35]. The number of wind power samples needed to give a good representation of the uncertainty is investigated in [45], in this case study we use 30 wind power samples as more samples increase the solution time without significant improvements of the solution.

4. Results

The regional power system is almost in net balance with respect to the annual energy use versus production, thus the total costs are mainly determined by the regulating costs. As regulating penalties occur when using any resource to react to deviations from expected wind power production, which are the same for all cases, there are only small differences of 1.7-3.4 % in the total costs of the system for the different levels of hydro power flexibility. These differences are mainly due to the fact that more energy is wasted when hydro power is less flexible and can't react to unforeseen wind power, which leads to more spillage and curtailment as seen in Figure 7 for the low regulating price. For increasing hydro power flexibility the total amount of wasted energy is substantially decreased, compared to the worst case with no hydro power flexibility the energy waste is reduced by 28 % and 56 % when increasing the flexibility to 6 and 24 hours. The increase in wasted energy due to higher regulation prices is smaller and range from 2-9 %.

The total amount of regulating power needed to balance the system is the same in all the cases, the main difference are how the regulating power is distributed between the different hydro

Table 3: Line reactance and capacities for the case system, including an adjustment factor for line capacity compared to a deterministic sizing model.

Line	0, 1	1, 2	2, 3	3, 4	3, 5	4, 7	5, 6	5, 7	7, 8	8, 9
Reactance [p.u]	0.027	0.035	0.046	0.075	0.076	0.147	0.028	0.031	0.048	0.047
Capacity [MW]	307.5	359.0	433.0	109.8	324.8	109.8	426.6	523.6	439.2	411.4
Cap Increase	1.5	2.0	2.0	1.0	1.5	1.0	1.0	2.0	2.0	2.0

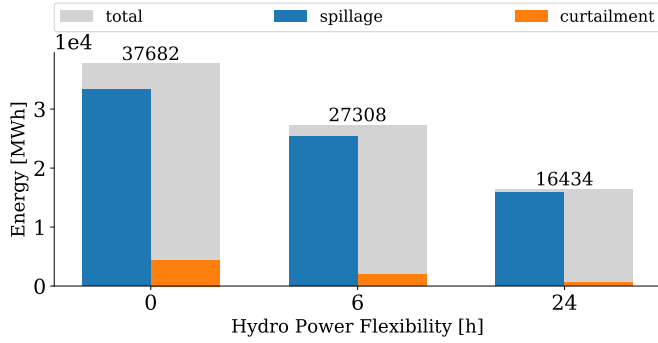


Figure 7: Energy wasted by spilling water from hydro power or curtailing wind power over the year for the low regulating price. Energy wasted in a model with perfect foresight of wind power production is subtracted from these numbers

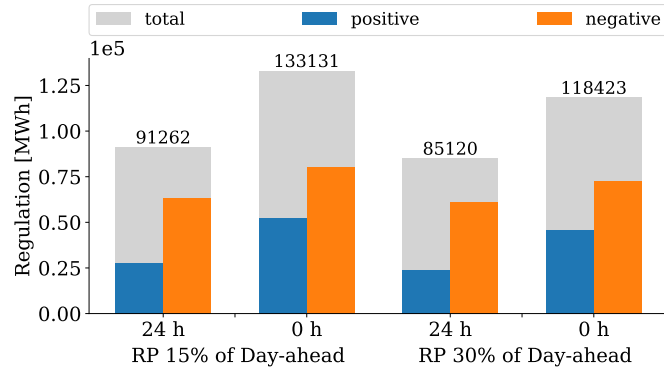


Figure 8: Regulation by the hydrogen plant for different levels of hydro power flexibility and regulation price

power plants and the electrolysis. In the low hydro power flexibility case, hydro power is still used for regulation, but at higher costs as the reservoir levels are deviating from the reservoir guide curve resulting in penalties. A significant shift of regulating power from the hydro power plants to the electrolysis is observed when the hydro power flexibility is reduced as shown in Figure 8. The increase in regulating power from the electrolysis as a result of less hydro power flexibility is 39-46 %. Increasing the regulating price results in a reduced amount of regulating power delivered by the electrolysis plant of 7-11 %.

Figure 9 and 10 shows duration curves for electrolysis power and storage level, in duration curves the values are sorted from highest to lowest, this gives a indication on how the components are operating. The two most common operational states of the electrolysis plant is either to operate at maximum capacity or to supply the hydrogen load directly by producing the exact amount of hydrogen required, as illustrated by the flat parts of the duration curve in Figure 9. The electrolysis pro-

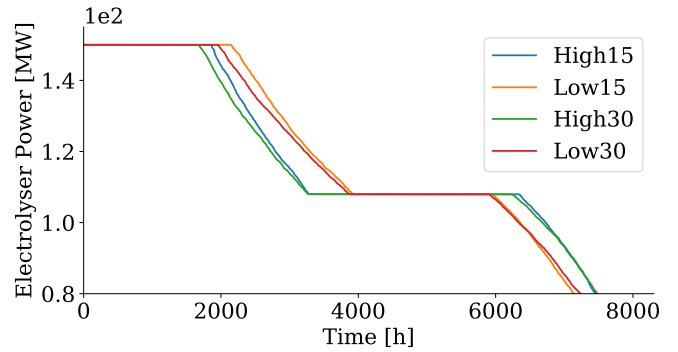


Figure 9: Duration curves for the electrolysis power for high and low hydro power flexibility and regulating prices of 15 and 30 % of the day-ahead price

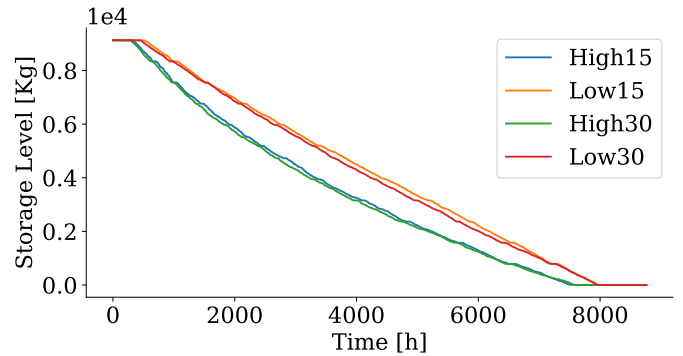


Figure 10: Duration curves for the hydrogen storage for high and low hydro power flexibility and regulating prices of 15 and 30 % of the day-ahead price

duce more hydrogen directly to the hydrogen load when hydro power can deliver flexibility as this is more efficient by avoiding compression to higher pressures.

The operation on high power levels increase when hydro power is less flexible and the electrolysis has to deliver a higher share of the regulating power. More hydrogen is produced to the hydrogen storage to be able to react to unforeseen wind power production, or lack thereof. The higher storage utilization can be observed in Figure 10, where the area under the duration curve is larger. The storage is more utilized at all levels, but especially on intermediate levels to allow for both up and down regulation. From Figure 9, we see that when the regulating price is high then the electrolysis produce less the top the power levels as it is expensive to regulate and energy is rather curtailed or spilled. As a result the utilization of the hydrogen storage is also slightly reduced for increasing regulating prices.

In Figure 11 we compare the feedstock costs, i.e. cost of electricity for hydrogen production, from the cases with the DOE targets for large scale hydrogen production in 2015 and 2020. In recent NREL cases for hydrogen production, feedstock in

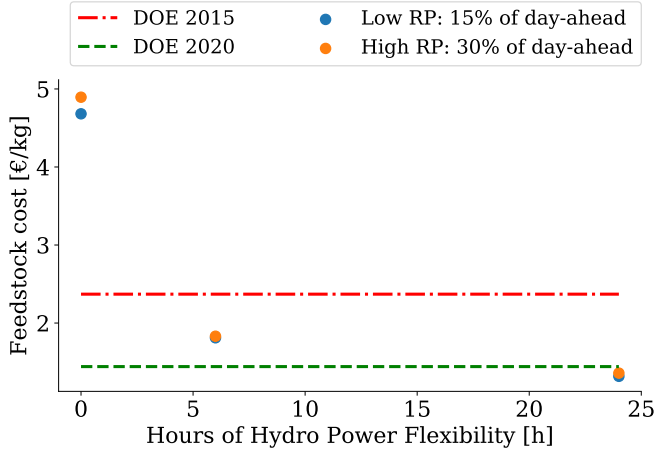


Figure 11: Cost of producing hydrogen compared to the DOE targets for 2015 and 2020, the targets are converted from 2007 to 2015 values to adjust for inflation [46]

PEM electrolysis currently estimated to represent around 77 % of the cost of hydrogen production at about 3.60 €/kg. In areas with large amount of renewables the feedstock costs can be significantly lower, specially if there is hydro power for balancing the natural variability in renewable power output. Flexible hydro power production contributes to significantly lowering the feedstock costs, going from 0 to 6 hours of flexibility results is a large drop in production costs while going from 6 to 24 hours gives a smaller but still very significant cost reductions of about 27 %. The lowest cost is about 1.32 €/kg for the low regulating price, which is lower than the 2020 DOE targets at 1.46 €/kg (adjusted for inflation to 2015 values [46]). The feedstock cost is calculated by using the dual value of the hydrogen balance in Equation 7, this value represent the marginal cost of producing one more unit of hydrogen to the power system at the location of the electrolysis plant in bus 6. From the dual value of Equation 8, we get a corresponding average electricity price of 25.6 €/MWh in bus 6, as a point of reference the historical average of the energy price in this area was 30.82 €/MWh from 2013 to 2019. The increase in feedstock costs for higher regulating prices are about 1-5 %.

It should be noted that in all cases the reservoir levels have some deviations from the reservoir guiding curves at the fixed points, which affects the cost of hydrogen production. The reservoir deviation penalty is set by trial and error to be 50 €/MWh and is a signal designed to affect the hydro power strategy without any direct physical meaning. However, it can also be interpreted as high regulation cost for the hydro power plants when they deliver additional regulation compared to what the flexibility in each case allow.

Increasing the installed capacities of wind power, transmission lines, hydro power generators, reservoirs, electrolysis or hydrogen storage can further reduce the feedstock costs but this has to be investigated using an investment model that considers the capital costs of the different technologies against the operational benefits. The sensitivity of the feedstock cost to changes in electrolysis capacity and hydrogen storage is shown in Fig-

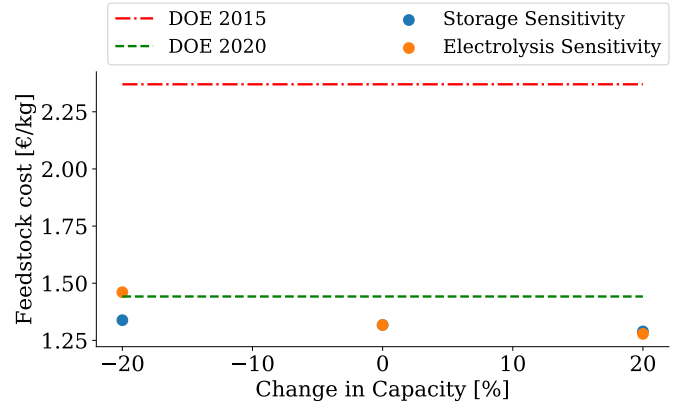


Figure 12: Sensitivities of the feedstock cost for hydrogen production from changing the storage and electrolysis capacity respectively. Based on the case with 24 hours of hydro power flexibility that gives the cheapest electrolysis feedstock costs.

Table 4: Cost of hydrogen production for the case with high levels of hydro power flexibility, using current and future estimates of capital and fixed O&M costs.

	Current	Future	DOE - 2020
Capital [€/kg]	0.72	0.31	0.41
Feedstock [€/kg]	1.32	1.32	1.46
Fixed O&M [€/kg]	0.53	0.26	0.21
Total [€/kg]	2.57	1.89	2.08

ure 12 for the case with the lowest hydrogen feedstock costs. The differences in feedstock costs when changing the hydrogen storage with +/- 20 % is about 2% in either direction. Reducing the electrolysis capacity by 20% have a more significant effect with a 11 % increase in the feedstock costs, while 20 % more capacity only gives a 3 % reduction in feedstock costs.

If we use the excel tool from the NREL analysis [2] and oversize the electrolysis plant to fit our case study with a capacity of (150 MW / 51.84 kWh/kg) · 24 h/day = 70 ton/day, we get the capital costs and fixed O&M costs shown in Table 4. In the capital cost we also include an additional 0.02 €/kg for the hydrogen storage [29]. The costs are calculated for two cases, where the main difference is the electrolysis stack cost of 810 and 360 €/kWh for the current and future case respectively. Using the feedstock cost from this analysis we get a total cost of hydrogen production of 2.57 and 1.89 €/kg for the present or future case respectively. As seen from the results, using the current investment cost results in total cost higher than the DOE target while future costs results in total costs below the DOE target. This is still higher than reported cost estimates for hydrogen produced from natural gas with carbon sequestration at 1.56 \$/kg or 1.41 €/kg, which doesn't include the cost of carbon storage. This shows that with high levels of wind penetration electrolysis can get close to the costs of hydrogen production from natural gas in the future. There is however, several factors that has to be considered further by performing an investment analysis, such as the cost of carbon storage and how much wind power it is economical to integrate before lower electricity prices makes it unprofitable.

5. Conclusion

In this work we present a model for optimizing the operation of a region in the power system with high wind power penetration and large scale hydrogen production. The model takes into consideration power flow, energy storage and short-term uncertainty from wind power. The model is based on a rolling horizon framework, use scenarios to represent wind power uncertainty and guiding curves for long-term energy storage strategies.

The value of flexible hydro power on the cost of hydrogen production from electrolysis is investigated in a case study of a future scenario of the power system in the Finnmark region in northern Norway. The flexibility from hydro power is quantified by allowing the reservoir level to deviate from the guiding curve within a time range of 0, 6 or 24 hours. The case study shows how the system is affected by the presence of flexibility from hydro power and how the electrolysis plant increasingly delivers flexibility when the hydro power has a tight operating range.

Increasing levels of hydro power flexibility reduces the lost energy in the system by up to 56 % with 24 hours of flexibility compared to no flexibility. Low hydro power flexibility in the 0 hours case causes the amount of regulation delivered by the electrolysis to increase by up to 39-46 % compared to when hydro power has high flexibility in the 24 hours case.

The case study shows that flexibility from hydro power is important for the cost of hydrogen production in power systems with high levels of wind power penetration. Increasing the time range in which the reservoir level can deviate from the guiding curve from 6 to 24 hours results in a reduction in cost from electricity consumption for the electrolysis of 27 %, from 1.83 to 1.32 €/kg. The lowest total costs at 1.89 €/kg are fulfilling the US Department of Energy targets for large scale hydrogen production in 2020, and is close to competing with hydrogen production from natural gas with carbon sequestration which is estimated at 1.41 €/kg. It should be noted that our results are obtained using regulating power price premiums of 15 and 30 % of the day-ahead price which is higher than observed in the market today.

Significant modifications to the installed capacities found by a deterministic investment model had to be made to make the stochastic case study feasible. This shows that short term uncertainty should be taken into account when making investments in systems with high amount of wind power. In future work the model presented here will be expanded to an investment model. Additionally the effect of penalties from the guiding curve deviations will be studied more in detail and other methods for representing the hydro power flexibility that has lower or more economically correct impact on the objective and dual values will be tested.

6. Acknowledgements

This publication is based on results from the research project Hyper, performed under the ENERGIX programme. The authors acknowledge the following parties for financial support:

Equinor, Shell, Kawasaki Heavy Industries, Linde Kryotechnik, Mitsubishi Corporation, Nel Hydrogen and the Research Council of Norway (255107/E20). The authors would also like to thank Prof. Øivind Wilhelmsen at SINTEF and NTNU for feedback on this manuscript.

7. References

- [1] Iea, Technology Roadmap Hydrogen and Fuel Cells, Tech. rep. (2015).
- [2] National Renewable Energy Laboratory, H2A: Hydrogen Analysis Production Case Studies — Hydrogen and Fuel Cells — NREL. URL <https://www.nrel.gov/hydrogen/h2a-production-case-studies.html>
- [3] A. Ursua, L. Gandia, P. Sanchis, Hydrogen Production From Water Electrolysis: Current Status and Future Trends, Proceedings of the IEEE 100 (2) (2012) 410–426. doi:10.1109/JPROC.2011.2156750.
- [4] REFHYNE Clean Refinery Hydrogen for Europe. URL <https://refhyne.eu/>
- [5] O. Ulleberg, T. Nakken, A. Ete, The wind/hydrogen demonstration system at Utsira in Norway: Evaluation of system performance using operational data and updated hydrogen energy system modeling tools, International Journal of Hydrogen Energy 35 (5) (2010) 1841–1852. doi:10.1016/j.ijhydene.2009.10.077.
- [6] M. d. P. Argumosa, B. Simonsen, S. Schoenung, Evaluations of hydrogen demonstration projects, International Energy Agency (2010) 1–35.
- [7] B. Lyseng, T. Niet, J. English, V. Keller, K. Palmer-Wilson, B. Robertson, A. Rowe, P. Wild, System-level power-to-gas energy storage for high penetrations of variable renewables, International Journal of Hydrogen Energy 43 (4) (2018) 1966–1979. doi:10.1016/J.IJHYDENE.2017.11.162.
- [8] C. J. Greiner, M. Korpås, A. T. Holen, A Norwegian case study on the production of hydrogen from wind power, International Journal of Hydrogen Energy 32 (10) (2007) 1500–1507. doi:10.1016/j.ijhydene.2006.10.030.
- [9] M. Korpås, C. J. Greiner, Opportunities for hydrogen production in connection with wind power in weak grids, Renewable Energy 33 (6) (2008) 1199–1208. doi:10.1016/j.renene.2007.06.010.
- [10] C. J. Greiner, M. Korpås, T. Gjengedal, A Model for Techno-Economic Optimization of Wind Power Combined with Hydrogen Production in Weak Grids, EPE Journal 19 (2) (2009) 52–59. doi:10.1080/09398368.2009.11463717.
- [11] Statkraft, Energy solution: Renewable proposal for Svalbard — Explained. URL <https://explained.statkraft.com/articles/2018/energy-solution-renewable-proposal-for-svalbard/>
- [12] S. M. Saba, M. Müller, M. Robinius, D. Stolten, The investment costs of electrolysis A comparison of cost studies from the past 30 years, International Journal of Hydrogen Energy 43 (3) (2018) 1209–1223. doi:10.1016/J.IJHYDENE.2017.11.115.
- [13] J. I. Levene, M. K. Mann, R. M. Margolis, A. Milbrandt, An analysis of hydrogen production from renewable electricity sources, Solar Energy 81 (6) (2007) 773–780. doi:10.1016/J.SOLENER.2006.10.005.
- [14] United States Department of Energy, Hydrogen Production, Fuel Cell Technologies Office Multi-Year Research, Development and Demonstration Plant 11007 (2015) 1–44. doi:10.2172/1219578.
- [15] IRENA, Renewable Power Generation Costs in 2017, Abu Dhabi, 2018.
- [16] F. R. Førstund, B. Singh, T. Jensen, C. Larsen, Phasing in wind-power in Norway: Network congestion and crowding-out of hydropower, Energy Policy 36 (2008) 3514–3520. doi:10.1016/j.enpol.2008.06.005.
- [17] X. Lu, M. B. McElroy, W. Peng, S. Liu, C. P. Nielsen, H. Wang, Challenges faced by China compared with the US in developing wind power, Nature Energy 1 (6) (2016) 16061. doi:10.1038/nenergy.2016.61.
- [18] L. Welder, P. Stenzel, N. Ebersbach, P. Markewitz, M. Robinius, B. Emonts, D. Stolten, Design and evaluation of hydrogen electricity reconversion pathways in national energy systems using spatially and temporally resolved energy system optimization, International Journal of Hydrogen Energy 44 (19) (2019) 9594–9607. doi:10.1016/J.IJHYDENE.2018.11.194.

- [19] Y. Jiang, B. Wen, Y. Wang, Optimizing unit capacities for a wind-hydrogen power system of clustered wind farms, *International Transactions on Electrical Energy Systems* 29 (2) (2019) e2707. doi:10.1002/etep.2707.
- [20] T. Grube, L. Doré, A. Hoffrichter, L. E. Hombach, S. Raths, M. Robinius, M. Nobis, S. Schiebahn, V. Tietze, A. Schnettler, G. Walther, D. Stolten, An option for stranded renewables: electrolytic-hydrogen in future energy systems, *Sustainable Energy & Fuels* 2 (7) (2018) 1500–1515. doi:10.1039/C8SE00008E.
- [21] B. Olateju, A Techno-Economic Assessment of Sustainable Large Scale Hydrogen Production from Renewable and Non-Renewable Sources doi: 10.7939/R33F4KW3X.
- [22] G. Zhang, X. Wan, A wind-hydrogen energy storage system model for massive wind energy curtailment, *International Journal of Hydrogen Energy* 39 (3) (2014) 1243–1252. doi:10.1016/J.IJHYDENE.2013.11.003.
- [23] B. Nastasi, G. Lo Basso, Hydrogen to link heat and electricity in the transition towards future Smart Energy Systems, *Energy* 110 (2016) 5–22. doi:10.1016/J.ENERGY.2016.03.097.
- [24] P. D. Lund, J. Lindgren, J. Mikkola, J. Salpakari, Review of energy system flexibility measures to enable high levels of variable renewable electricity, *Renewable and Sustainable Energy Reviews* 45 (2015) 785–807. doi:10.1016/J.RSER.2015.01.057.
- [25] P. Meibom, R. Barth, B. Hasche, H. Brand, C. Weber, M. O’Malley, Stochastic optimization model to study the operational impacts of high wind penetrations in Ireland, *IEEE Transactions on Power Systems* 26 (3) (2011) 1367–1379. doi:10.1109/TPWRS.2010.2070848.
- [26] M. Korpås, A. T. Holen, Operation planning of hydrogen storage connected to wind power operating in a power market, *IEEE Transactions on Energy Conversion* 21 (3) (2006) 742–749. doi:10.1109/TEC.2006.878245.
- [27] Y. Wang, Z. Zhou, A. Botterud, K. Zhang, Q. Ding, Stochastic coordinated operation of wind and battery energy storage system considering battery degradation, *Journal of Modern Power Systems and Clean Energy* 4 (4) (2016) 581–592. doi:10.1007/s40565-016-0238-z.
- [28] A. Helseth, A. Gjelsvik, B. Mo, . Linnet, A model for optimal scheduling of hydro thermal systems including pumped-storage and wind power, *IET Generation, Transmission & Distribution* 7 (12) (2013) 1426–1434. doi:10.1049/iet-gtd.2012.0639.
- [29] E. F. Bødal, M. Korpås, Production of Hydrogen from Wind and Hydro Power in Constrained Transmission grids, Considering the Stochasticity of Wind Power, *Journal of Physics: Conference Series* 1104 (1) (2018) 012027. doi:10.1088/1742-6596/1104/1/012027.
- [30] Norwegian Meteorological Institute, TdsStaticCatalog <http://thredds.met.no/thredds/metno.html>.
URL <http://thredds.met.no/thredds/metno.html>
- [31] The Norwegian Water Resources and Energy Directorate, Wind power. URL <https://www.nve.no/energiforsyning-og-konsesjon/vindkraft/?ref=mainmenu>
- [32] J. B. Bremnes, A comparison of a few statistical models for making quantile wind power forecasts, *Wind Energy* 9 (1-2) (2006) 3–11. doi:10.1002/we.182.
- [33] R. Koenker, *Fundamentals of Quantile Regression*, in: *Quantile Regression*, Cambridge University Press, 2005, Ch. Fundamenta.
- [34] P. Pinson, H. Madsen, G. Papaefthymiou, From Probabilistic Forecasts to Statistical Scenarios of Short-term Wind Power Production, *WIND ENERGY* Wind Energ 12 (2009) 51–62. doi:10.1002/we.284.
- [35] K. Skytte, P. E. Grohnheit, *Market Prices in a Power Market with More Than 50% Wind Power*, Springer, Cham, 2018, pp. 81–94. doi:10.1007/978-3-319-74263-2{_}4.
- [36] K. Skytte, The regulating power market on the Nordic power exchange Nord Pool: an econometric analysis, *Energy Economics* 21 (4) (1999) 295–308. doi:10.1016/S0140-9883(99)00016-X.
- [37] S. Stage, Y. Larsson, Incremental Cost of Water Power, *Transactions of the American Institute of Electrical Engineers. Part III: Power Apparatus and Systems* 80 (3) (1961) 361–364. doi:10.1109/AIEEPAS.1961.4501045.
- [38] J. Lindqvist, Operation of a Hydrothermal Electric System: A Multistage Decision Process, *Power Apparatus and Systems, Part III. Transactions of the American Institute of Electrical Engineers* 81 (April) (1962) 1–6.
- [39] B. Stott, J. Jardim, O. Alsac, DC Power Flow Revisited, *IEEE Transactions on Power Systems* 24 (3) (2009) 1290–1300. doi:10.1109/TPWRS.2009.2021235.
- [40] The Norwegian Water Resources and Energy Directorate, Norwegian Power System. URL <https://www.nve.no/map-services/?ref=mainmenu>
- [41] Statistics Norway, Net consumption of electricity, by consumer group (GWh) (M) 2010 - 2017. Statbank Norway. URL <https://www.ssb.no/en/statbank/table/10314/>
- [42] Nordpool, Historical Market Data. URL <https://www.nordpoolgroup.com/historical-market-data/>
- [43] E. F. Bødal, M. Korpås, Regional Effects of Hydrogen Production in Congested Transmission Grids with Wind and Hydro Power, in: *14th International Conference on the European Energy Market - EEM, IEEE, 2017*, pp. 1–6. doi:10.1109/EEM.2017.7982013.
- [44] M. Ozaki, S. Tomura, R. Ohmura, Y. H. Mori, Comparative study of large-scale hydrogen storage technologies: Is hydrate-based storage at advantage over existing technologies?, *International Journal of Hydrogen Energy* 39 (7) (2014) 3327–3341. doi:10.1016/j.ijhydene.2013.12.080.
- [45] E. F. Bødal, M. Korpås, Value of Hydro Power Flexibility for Hydrogen Production in Constrained Transmission Grids [Under review], *International Journal of Hydrogen Energy*.
- [46] U.S. Bureau of Labor Statistics, CPI Inflation Calculator. URL https://www.bls.gov/data/inflation_calculator.htm